J Solid State Electrochem (2010) 14:2153–2159
DOI 10.1007/s10008-010-1099-4

ORIGINAL PAPER

Characteristics of methyl cellulose-NH_4NO_3-PEG electrolyte and application in fuel cells

N. E. A. Shuhaimi · N. A. Alias · M. Z. Kufian · S. R. Majid · A. K. Arof

Received: 20 January 2010 / Revised: 3 May 2010 / Accepted: 10 May 2010 / Published online: 29 June 2010

Abstract We report the viability of methyl cellulose (MC) as a membrane in a polymer electrolyte membrane fuel cell (PEMFC). Methyl cellulose serves as the polymer host, ammonium nitrate (NH_4NO_3) as the doping salt and poly (ethylene glycol) (PEG) as plasticizer. Conductivity measurement was carried out using electrochemical impedance spectroscopy. The room temperature conductivity of pure MC film is $(3.08 \pm 0.63) \times 10^{-11}$ S cm^{-1}. The conductivity increased to $(2.10 \pm 0.37) \times 10^{-6}$ S cm^{-1} on addition of 25 wt.% NH_4NO_3. By adding 15 wt.% of PEG 200 to the highest conducting sample in the MC-NH_4NO_3 system, the conductivity was further raised by two orders of magnitude to $(1.14 \pm 0.37) \times 10^{-4}$ S cm^{-1}. The highest conducting sample containing 15 wt.% PEG was used as membrane in PEMFC and was operated at room and elevated temperatures. From voltage-current density characteristics, the short circuit current density was 31.52 mA cm^{-2} at room temperature (25 °C).

Keywords Methyl cellulose · Ammonium nitrate · Poly (ethylene glycol) · Fuel cells

Introduction

A polymer electrolyte membrane fuel cell (PEMFC) is a 'green' device since it produces electricity through electrochemical reaction and water as the by-product. Among the fuel cell membranes representing the-state-of-the-art include fluorinated ionomers and its complexes, high-molecular/low-molecular composite membranes and organic/inorganic composite membranes [1]. Although these materials may exhibit good chemical stability and excellent performance [2, 3] when applied in membrane fuel cells, they are not without disadvantages. Some of the disadvantages include high cost [4], limited oxidation stability, complicated production process, and difficult sulfonation and phosphonation procedures as exemplified by ionomer types based on poly (α, β, β-triflurostyrene)–homopolymer and copolymers and strong swelling in polymer with arylene main chain polymers which, after a certain degree of sulfonation or when a certain operating temperature is exceeded will experience a decrease in mechanical stability [1]. Nafion is known to give high proton conductivity at low temperature and under high humidity conditions. Hence, the disadvantage of Nafion is also the requirement of humidification during operation of fuel cells [5, 6]. The production process using Nafion is also environmental unfriendly [7].

Apart from these materials, polymers such as chitosan [8, 9], poly (vinylidene fluoride-hexafluropropylene) (PVdF-HFP) [10] and poly(vinyl alcohol) (PVA) [11] have been used or suggested as membranes for fuel cells. Composite membranes have been prepared using chitosan as the matrices and potassium hydroxide as the doping salt [12]. The fuel cells showed an open-circuit voltage of ~1.0 V and a current density of ~30 mA cm^{-2}. Cross-linked quarternized-chitosan membranes [13] exhibited a current density of 65 mA cm^{-2} at a temperature of 50 °C. PVA-KOH electrolyte membrane has been used in direct methanol fuel cell which could deliver an initial power density of ~10 mW cm^{-2} at 90 °C [11].

In this work, we have prepared and characterized a new polymer electrolyte based on MC, which is doped with ammonium nitrate (NH_4NO_3) and plasticized with poly

N. E. A. Shuhaimi · N. A. Alias · M. Z. Kufian · S. R. Majid · A. K. Arof (✉)
Center for Ionics University of Malaya (CIUM),
Department of Physics, Faculty of Science, University of Malaya,
50603 Kuala Lumpur, Malaysia
e-mail: akarof@um.edu.my

(ethylene glycol) (PEG). The experiments carried out in this study include X-ray diffraction to determine whether the films are amorphous or crystalline and electrochemical impedance spectroscopy to obtain the conductivity of MC-based polymer electrolytes. The highest conducting sample will be used as a membrane in a PEMFC and characteristics of the fuel cell studied using the Autolab PGSTAT 12 potentiostat.

Experimental

Preparation of MC-based polymer electrolytes

Preparations of the MC-based films were carried out by solution casting technique. MC consists of ß (1→4) glucosidic units with methyl substituents in linear chains [14] and has polar groups at oxygen atoms which can act as electron donors. MC has attracted much interest because it is biodegradable [15], cheap [15], non-toxic [16], has good mechanical strength [17], and excellent film forming ability [18]. MC has been used as a dispersing and thickening agent in the food industry [19]. The use of MC in these activities depends on its solubility in water and level of methoxy substitution on the cellulose chain [20]. MC was dissolved in distilled water until a clear viscous solution was obtained. Desired amounts of NH_4NO_3 were added and stirred until complete dissolution of the salt. The highest conducting polymer-salt film contains 25 wt.% of NH_4NO_3. To this, different amounts of PEG (200) were added. The solutions were poured into different plastic Petri dishes at room temperature for films to form. After drying, the samples were kept in a dry box.

Characterization of polymer electrolytes

The nature of MC-based polymer electrolytes was investigated using Siemens D5000 X-ray diffractometer at 2θ angles in the range from 5º to 80º. The operating current was 40 mA and operating voltage, 40 kV. Step size for MC-doped NH_4NO_3 was 0.1º and for plasticized polymer electrolytes was 0.05º.

The surface morphology of MC-based polymer electrolytes were studied using Field Emission Scanning Electron Microscope (FEI Quanta 200 F). To measure the conductivity, impedance measurement was performed with the HIOKI 3531-01 LCR bridge at room temperature (25 °C) to 100 °C in the frequency range 50 Hz to 1 M Hz. The membrane was sandwiched between two stainless steel electrodes.

PEMFC fabrication

The PEMFC® kit was purchased from H-Tec (Germany). The electrode area is 16 cm^2. At the anode, hydrogen gas that enters the anode is atomized and oxidized. The oxidized hydrogen atoms or protons diffuse into the proton conducting polymer electrolyte. The oxygen in the air that enters the cathode is reduced by electrons that enter the cathode from the external circuit. The reduced oxygen combines with the protons to form water. To make a good electrode/electrolyte contact in the membrane electrode assembly (MEA), the membrane was soaked in 1% orthophosphoric acid [21]. To test the performance of the PEMFC at selected temperatures, the assembled fuel cell was placed in a chamber which was attached with a digital thermocouple. A hot air blower was used to increase and maintain the temperature until measurements have been carried out. The temperature was raised and measurements were repeated for the desired number of times. The H_2 flow rate from the tank to the cell was 0.5 L/min and H_2 pressure was 0.6 bars. Current-potential (*I-V*) characteristics were measured using Autolab PGSTAT 12 potentiostat.

Energy dispersive analysis of X-rays for fuel cell electrode

Energy dispersive analysis of X-rays (EDX) of the electrodes were also taken to determine the elements present in the anode (where hydrogen enters the cell) and cathode (where air enters the cell).

Results and discussion

MC-NH_4NO_3 system

Figure 1 depicts image from scanning electron microscope taken at ×2,000 magnification. Samples doped with 25 wt.% of NH_4NO_3 and less has a smooth surface while sample with 30 wt.% NH_4NO_3 exhibits a rough surface probably due to recrystallization of salt at the surface of the polymer. This is supported by results from XRD that show peaks due to NH_4NO_3 in the diffractogram for the sample containing 30 wt.% salt [22]. The recrystallization of the salt out of the bulk of the sample reduces the number of mobile ions inside the sample and hence the conductivity.

For samples of different polymer-salt composition in the MC-NH_4NO_3 systems, the highest conducting sample at room temperature has composition 75 wt.% MC and 25 wt.% NH_4NO_3. The conductivity is 2.10×10^{-6} cm^{-1}. This sample and those containing less than 25 wt.% salt are amorphous. Samples with higher salt concentration (>25 wt.%) show peaks due to NH_4NO_3. Details can be found in our previous paper [22]. This value is quite comparable to conductivity of other electrolytes containing ammonium salt as dopant. Khiar et al. [23] studied the conductivity of chitosan doped with $NH_4CF_3SO_3$ and found that the highest conducting sample has conductivity 1.5×

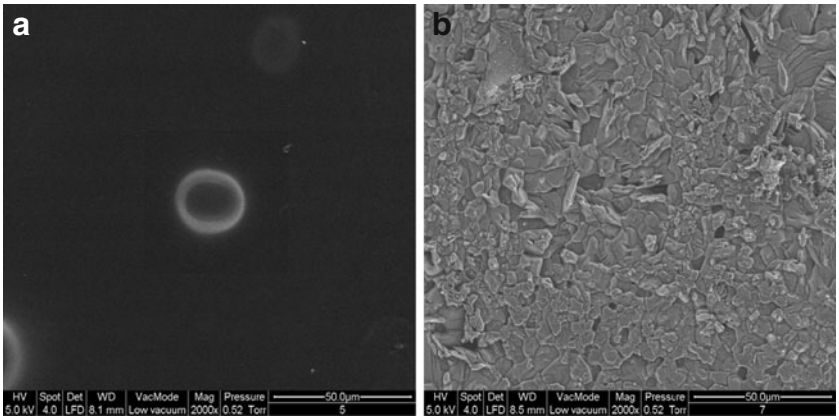

Fig. 1 SEM image of **a** MC doped with 25 wt.% of NH_4NO_3 and **b** MC doped with 30 wt.% of NH_4NO_3

10^{-6} S cm^{-1} at 303 K for 50 wt.% chitosan and 50 wt.% $NH_4CF_3SO_3$. Hirankumar et al. [24] reported the highest conductivity for PVA doped with NH_4CH_3COO is 1.1×10^{-6} S cm^{-1} at 303 K.

Figure 2 shows temperature dependence of conductivity for highest conducting sample in the MC-NH_4NO_3 system. Each point is the average of three conductivity values. From the figure, it can be observed that the conductivity increases with temperature up to 60 °C, after which conductivity decreases. These results indicate that 75 wt.% MC-25 wt.% NH_4NO_3 is not suitable for use in PEMFC despite its higher room temperature conductivity over recast Nafion [25].

According to Sarkar [26], at low temperatures and in the solution state, MC molecules can be easily hydrated. Hence, when the MC-salt solution forms film at room temperature, it is expected to contain water. Although it has been kept in the desiccators for purpose of continuous drying, there is still possibility that the film contains water. As the temperature is increased during conductivity-temperature measurements, the water molecules are gradually removed and hence the number density of hydroxonium ions is reduced leading to a drop in the rate of increase in conductivity between 25 °C and 60 °C. Above 60 °C, conductivity begins to drop probably due to increase in the rate of water loss that could also contain dissolved NH_4NO_3 in it.

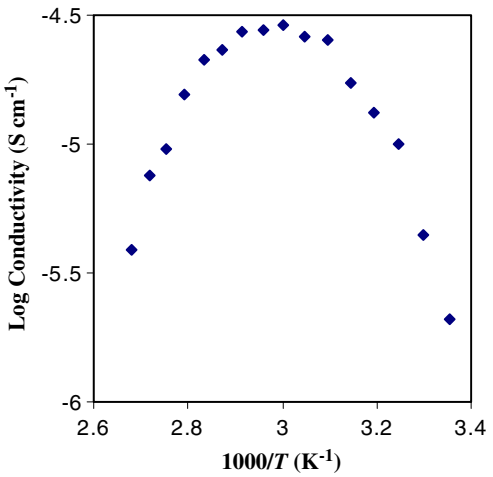

Fig. 2 Variation of ionic conductivity as a function of temperature for highest conducting sample in the MC-NH_4NO_3 system

MC-NH_4NO_3-PEG system

High conducting polymer electrolyte is very important for PEMFC fabrication. Ionic conduction occurs mainly in the amorphous phase [27]. The highest conducting sample from salted system, 75 wt.% MC-25 wt.% NH_4NO_3 was plasticized with different amounts of PEG. Pradhan et al. [28] pointed that the plasticizer should have low viscosity and high dielectric constant. The low viscosity will help to decrease the glass transition temperature, T_g and increase the amorphous content. The high dielectric constant of the plasticizer helps to dissociate the salt or ion aggregates. In the present study, PEG with low molecular weight (200) was used to enhance the conductivity of MC doped with NH_4NO_3. The viscosity of PEG (200) is 50 cP at 25 °C and its dielectric constant at 293 K is 19.95 but decreased to 18.41 at 303 K [29]. Awwad et al. reported the dielectric constant of PEG (200) as 18.43 at 303 K [30]. Park et al. [31] reported the ionic conductivity and relative permittivity for PEG/$LiClO_4$ complexes increased with decreasing molecular weight of PEG. Subban and co-workers [32] also reported similar observations when plasticizing PVC-$LiCF_3SO_3$ complexes with PEG of different molecular weights.

Figure 3 depicts X-ray diffraction for MC:NH_4NO_3-PEG system. It can be seen that, the 64 wt.% MC-21 wt.% NH_4NO_3-15 wt.% PEG is highly amorphous compared to samples containing other concentrations of PEG. This is based on the lower intensity of the peak at $2\theta=8°$ and an increase in broadness of the peak at $2\theta=21°$. On addition of more than 15 wt.% PEG to the highest conducting MC-NH_4NO_3 sample, a new peak was observed at $2\theta\approx 13°$ due to the formation of partially crystalline entities.

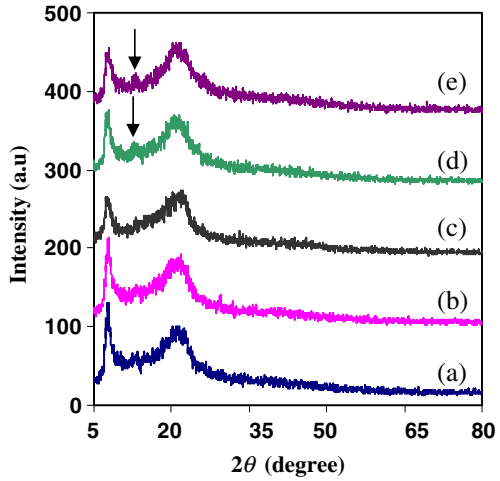

Fig. 3 X-ray diffraction patterns of **a** 71 wt.% MC-24 wt.% NH_4NO_3-5 wt.% PEG, **b** 68 wt.% MC-22 wt.% NH_4NO_3-10 wt.% PEG, **c** 64 wt.% MC-21 wt.% NH_4NO_3-15 wt.% PEG, **d** 60 wt.% MC-20 wt.% NH_4NO_3-20 wt.% PEG, and **e** 56 wt.% MC-19 wt.% NH_4NO_3 -25 wt.% PEG

Figure 4 shows the Cole-Cole plot of the highest conducting sample 64 wt.% MC-21 wt.% NH_4NO_3–15 wt.% PEG at room and elevated temperatures. The plot shows a low frequency spike suggesting that only capacitive component prevails in the polymer electrolytes. The bulk resistance was obtained from intercept at the *x*-axis as shown in the figure. Hence, conductivity of MC-based polymer electrolyte can be calculated after obtaining R_b using the equation below [33, 34]:

$$\sigma = \frac{d}{R_b A} \tag{1}$$

where, d is thickness, R_b is bulk resistance, and A is area of the sample.

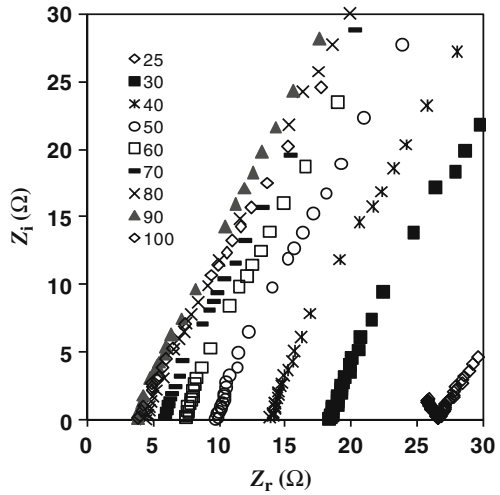

Fig. 4 Cole-Cole plot for highest conducting sample in MC-NH_4NO_3–PEG system

From Fig. 4, it is observed that, as the temperature increases, the bulk resistance decreases from 22.80 Ω at room temperature to 2.71 Ω at 100 °C. The parameter p of the CPE element increase with increasing the temperature from 0.70 at room temperature to 1.10 at 100 °C.

The use of PEG 200 is due to its lower glass transition temperature (T_g=−74 °C) compared to PEG 400, −62 °C and PEG 600, −50 °C. Ionic conductivity increases when the glass transition temperature decreases [35]. The lower glass transition temperature helps to increase the mobility of the ions and decrease the crystallinity of the polymer-salt complex [36]. The effect of PEG 200 on conductivity of MC-based polymer electrolytes is shown in Fig. 5. From Fig. 5, it can be observed that the conductivity increased from 2.10×10^{-6} S cm^{-1} for the 75 wt.% MC-25 wt.% NH_4NO_3 sample to 1.14×10^{-4} S cm^{-1} on addition of 15 wt.% PEG.

The conductivity value of the plasticized system in the present work is quite similar with that obtained by other researchers. Subban et al. [32] obtained the highest conductivity of 1.03×10^{-4} S cm^{-1} for the sample with composition 58 wt.% PVC-32 wt.% $LiCF_3SO_3$-10 wt.% PEG. Srivastava and Chandra [37] obtained conductivity approaching 10^{-4} S cm^{-1} for the sample 55 wt.% PESc-30 wt.% NH_4ClO_4-15 wt.% PEG. The increase in conductivity with increasing concentration of PEG as shown in Fig. 5 is attributed to the increase in number density and/or possibly ionic mobility of the charge carriers. Decrease in conductivity after 15 wt.% PEG is due to formation of partially crystalline entities as shown in X-ray diffractogram in Fig. 3.

Figure 6 depicts the temperature dependence of conductivity for the highest conducting sample in MC:NH_4NO_3-PEG system.

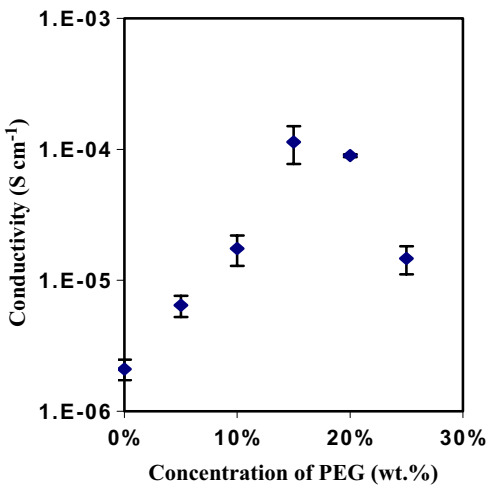

Fig. 5 Variation of ionic conductivity as a function of PEG concentration (wt.%)

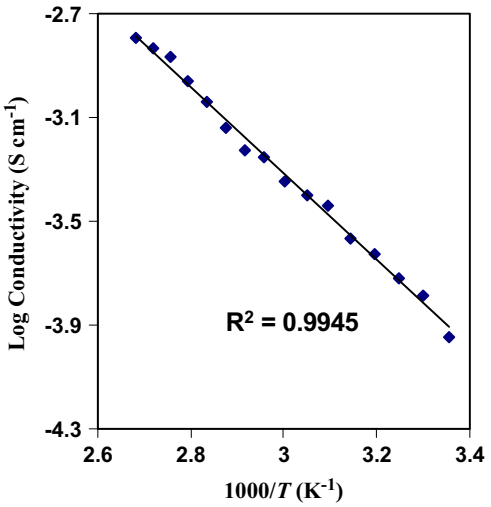

Fig. 6 Variation of ionic conductivity as a function of temperature for highest conducting sample in MC:NH_4NO_3-PEG system

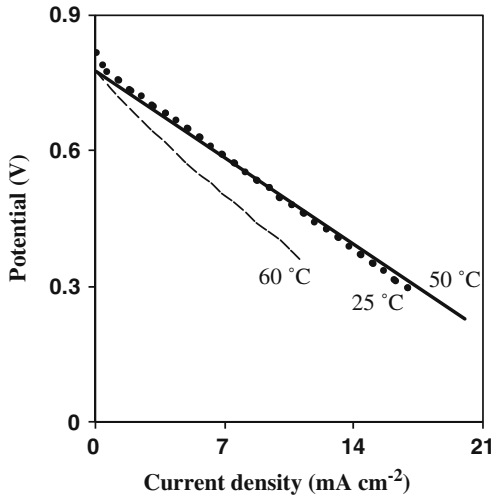

Fig. 7 Polarization curve of PEMFC using the highest conducting sample of MC:NH_4NO_3-PEG system

Unlike the conductivity-temperature relationship 75 wt.% MC-25 wt.% NH_4NO_3 sample, the conductivity increases with increase in temperature up to 100 °C. The regression value, R^2 was determined to be 0.99. The conductivity-temperature relationship exhibits Arrhenius-like behavior. According to Park and Ruckestein [17], among the many plasticizers for MC, PEG is the most suitable for the preparation of proton conducting electrolytes. This is because PEG is sufficiently hygroscopic enabling it to retain moderate moisture in the polymer and improves its flexibility without decreasing its mechanical strength. Therefore, the conductivity of the sample does not drop after 60 °C but continues to increase as temperature is increased to 100 °C. Hu et al. [25] have reported proton conductivity as a function of temperature for recast Nafion, Nafion-1.7 wt.% PBI-OO and Nafion-1.7 wt.% PBI-OO-0.5 wt.% nano-BN from 25 °C to 140 °C. PBI-OO is poly-[1-(4,4'-diphenylether)-5-oxybenzimidazole)-benzimidazole]. Comparing their report with the results in Fig. 6, it can be easily observed that the conductivity for 64 wt.% MC-21 wt.% NH_4NO_3 -15 wt.% PEG is much higher than that of reported by Hu et al. [25]. The results presented here is the average of six readings. As an example at 25 °C, the sample in the present investigation exhibits conductivity in the range 7.8×10^{-5} S cm^{-1} to 1.76×10^{-4} S cm^{-1} giving an average of 1.14×10^{-4} S cm^{-1} whereas the conductivity of recast Nafion is $\sim10^{-8}$ S cm^{-1}, Nafion-1.7 wt.% PBI-OO is $\sim10^{-6}$ S cm^{-1} and Nafion-1.7 wt.% PBI-OO-0.5 wt.% nano-BN is $\sim10^{-5}$ Scm^{-1}. At 100 °C, the conductivity of recast Nafion is $\sim10^{-6}$ S cm^{-1}, Nafion-1.7 wt.% PBI-OO is $\sim10^{-6}$ S cm^{-1} and Nafion-1.7 wt.% PBI-OO-0.5 wt.% nano-BN is $\sim10^{-5}$ S cm^{-1} which is still lower than that of the present sample which range from 3.23×10^{-4} S cm^{-1} to 3.08×10^{-3} S cm^{-1} giving an average of 1.60×10^{-3} S cm^{-1}. Since PEMFCs require high proton conducting membrane [38, 39], the MC-based proton conductor has potential for use as membrane in PEMFC due to its high conductivity at lower temperatures.

Table 1 EDX results for the electrode

Element	Element %	Atomic %
C	61.37	81.53
O	6.91	6.89
F	8.92	7.49
S	5.35	2.66
Pt	17.44	1.43
Total	100.00	100.00

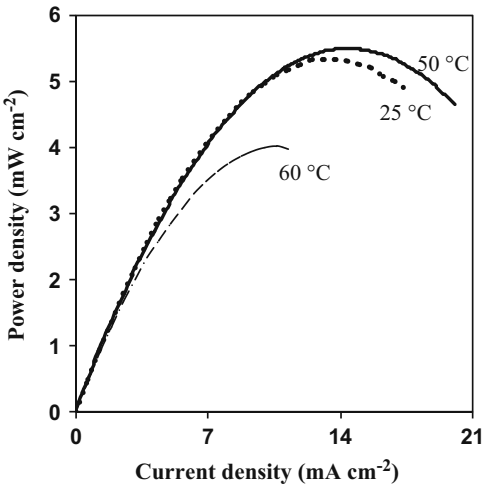

Fig. 8 Power density curve of PEMFC using the highest conducting sample of MC:NH_4NO_3-PEG system

Energy dispersive analysis of X-rays for fuel cell electrode

Table 1 lists the EDX result of the electrode after operation of the fuel cell. The results of EDX measurements showed the presence of elemental components such as Pt, C, and F in the MEA. These components are also present in the MEA reported by Hung et al. [40]. O observed is probably due to oxygen in methyl cellulose membrane stuck to the MEA electrolyte. The presence of Pt peaks at less than 5 keV and between 7 and 15 keV implies that the catalyst in the electrode is Pt.

PEMFC characteristics

PEMFC is commonly characterized by the cell efficiency, polarization curve, and power density variation with current density. In this work, the same sample 64 wt.% MC-21 wt.% NH_4NO_3-15 wt.% PEG was used as membrane in PEMFC, which was operated at temperatures (25 °C, 50 °C, and 60 °C successively). The minimum theoretical cell potential is 1.23 V [41]. PEMFC voltage efficiency was calculated using the equation below [42]:

$$\eta = \frac{\text{Actual voltage}}{\text{Theoretical voltage}} \times 100\% \quad (2)$$

The voltage efficiencies obtained in this work are 65%, 63%, and 62% for PEMFC operated at 25 °C, 50 °C, and 60 °C, respectively.

The polarization curve for the highest conducting sample in the MC:NH_4NO_3-PEG system is shown in Fig. 7. Increasing the operation temperature leads to decrease in open circuit potential (OCP). It can be observed in Fig. 7, the OCP at 25 °C is 0.82 V, at 50 °C is 0.78 V, and at 60 °C is 0.78 V. These results are similar to that reported by Zhang et al. [43]. The OCP was measured as a function of temperature and was found that for Nafion 112-based MEA, the OCP decrease from 1.01 V at 20 °C to 0.95 V at 120 °C. Meanwhile, for Nafion 117-based MEA, the OCP at 20 °C decrease with increasing temperature up to 120 °C from 1.04 V to 0.99 V. The short circuit current density (J_{sc}) at 25 °C is 30.3 mA cm^{-2}, at 50 °C is 31.5 mA cm^{-2} and at 60 °C is 23.49 mA cm^{-2}. Wan et al. [12] studied the viability of chitosan-based membranes doped with KOH in alkaline fuel cells at 50 °C and cut off voltage at 0.2 V, a current density ~17 mA cm^{-2} was obtained. In this work, at the same temperature, a current density of ~24 mA cm^{-2} was achieved at the same cut-off voltage.

Depicted in Fig. 8 is the performance of PEMFC based on power density curves. Peak power density at 25 °C is 5.34 mW cm^{-2}, at 50 °C is 5.51 mW cm^{-2}, and at 60 °C is 4.03 mW cm^{-2}.

From the graphs shown in Figs. 7 and 8, it can be seen that the performance of the MC-based membrane PEMFC is best at 50 °C. At 60 °C, the performance dropped. According to Bocchetta and co-workers [44], the increase in temperature results in decrease in OCP and J_{sc}. Their observations show that the solubility of their alumina membrane filled with phosphotungstic acid and Nafion® in the water produced at the cathode side increases with temperature. In the present work, MC, NH_4NO_3, and PEG were dissolved in water, there is possibility that the plasticized polymer dissolved in the reaction product.

This work has revealed the possibility of MC-based polymer electrolyte to be used as a membrane in fuel cell. However, further studies on water uptake, ion exchange capacity, and mechanical strength of the membrane need to be carried out.

Conclusions

MC-NH_4NO_3 and MC-NH_4NO_3-PEG electrolyte systems were prepared using solution casting technique. NH_4NO_3 is the proton provider. X-ray diffractogram shows that pure MC film is an amorphous polymer and all other samples show the same nature. Ionic conductivity of pure MC is 3.08×10^{-11} S cm^{-1} The conductivity increased up to 2.10×10^{-6} S cm^{-1} on addition of 25 wt.% NH_4NO_3. With addition of 15 wt.% PEG, conductivity was enhanced to 1.14×10^{-4} S cm^{-1}. The PEMFC fabricated using 64 wt.% MC-21 wt.% NH_4NO_3-15 wt.% PEG membrane achieved peak power of 5.51 mW cm^{-2} and short circuit current density is 31.5 mA cm^{-2} at temperature 50 °C.

Acknowledgments Authors are thankful to University of Malaya for providing financial support (PS223/2008C and PS312/2009C) and to the Ministry of Higher Education Malaysia (MOHE) for grant awarded (FP048/2008C) and permission to attend ABAF 10.

References

1. Kerres JA (2001) J Membr Sci 185:3–27
2. Liang H-Y, Qiu X-P, Zhang S-C, Zhu W-T, Chen L-Q (2004) J Appl Electrochem 34:1211–1214
3. Saccà A, Carbone A, Pedicini R, Portale G, D'Ilario L, Longo A, Martorana A, Passalacqua E (2006) J Membr Sci 278:105–113
4. Chen J, Asono M, Maekawa Y, Yoshida M (2006) J Membr Sci 277:249–257
5. Vona MLD, Marani D, D'Epifanio AD, Licoccia S, Beurroies I, Denoyel R, Knauth P (2007) J Membr Sci 304:76–81
6. Thomassin J-M, Kollar J, Caldarella G, Germain A, Jérôme R, Detrembleur C (2007) J Membr Sci 303:252–257
7. Pan H, Zhu X, Chen J, Jian X (2009) J Membr Sci 326:453–459
8. Wan Y, Peppley B, Creber KAM, Bui VT (2010) J Power Sources 195:3785–3793
9. Majid SR, Arof AK (2009) Polym Adv Tech 20:524–528

10. Kumar GG, Kim P, Nahm KS, Elizabeth RN (2007) J Membr Sci 303:126–131
11. Fu J, Qiao J, Wang X, Ma J, Okada T (2010) Synth Met 160:193–199
12. Wan Y, Peppley B, Creber KAM, Bui VT, Halliop E (2006) J Power Sources 162:105–113
13. Wan Y, Peppley B, Creber KAM, Bui VT, Halliop E (2008) J Power Sources 185:183–187
14. Garcìa MA, Pinotti A, Martino M, Zaritzky N (2009) Food Hydrocolloids 23:722–728
15. Rimdusit S, Jingjid S, Damrongsakkol S, Tiptipakorn S, Takeichi T (2008) Carbohydr Polym 72:444–455
16. Ye D, Montane D, Farriol X (2005) Carbohydr Polym 6:446–454
17. Park JS, Ruckestein E (2001) Carbohydr Polym 46:373–381
18. Lin SY, Wang SL, Wei YS, Li MJ (2007) Surf Sci 601:781–785
19. Luccia BHD, Kunkel ME (2002) Food Chem 77:139–146
20. Filho GR, de Assunção RMN, Vieira JG, da Meireles CS, Cerqueira DA, da Barud HS, Ribeiro SJL, Messaddeq Y (2007) Polym Degrad Stab 92:205–210
21. Lobato J, Cañizares P, Rodrigo MA, Linares JJ, Aguilar JA (2007) J Membr Sci 306:47–55
22. Shuhaimi NEA, Majid SR, Arof AK (2009) Mater Res Innovat 13:171–174, Special Issue
23. Khiar ASA, Puteh R, Arof AK (2006) Physica B 373:23–27
24. Hirankumar G, Selvasekarapandian S, Bhuvaneswari MS, Baskaran R, Vijayakumar M (2004) Ionics 10:135–138
25. Hu J, Luo J, Wagner P, Conrad O, Agert C (2009) Electrochem Commun 11:2324–2327
26. Sarkar N, Walker LC (1995) Carbohydr Polym 27:177–185
27. Awadhia A, Agrawal SL (2007) Solid State Ionics 178:951–958
28. Pradhan DK, Choudhary RNP, Samantaray BK (2009) Mater Chem Phys 115:557–561
29. Kinart CM, Klimczak M, Cwilinska A, Kinart WJ (2007) J Chem Thermodyn 39:822–826
30. Awwad AM, Al-Dujaili AA, Salman HE (2002) J Chem Eng Data 47:421–442
31. Park MK, Kim HS, An JH, Kim J (2005) J Ind Eng Chem 11:222–227
32. Subban RHY, Ahmad AH, Kamarulzaman N, Ali AMM (2005) Ionics 11:442–445
33. Hwang BJ, Liu YC, Lin HC (1997) J Polym Res 4:147–151
34. Baskaran R, Selvasekarapandian S, Hirankumar G, Bhuvaneswari MS (2004) Ionics 10:129–134
35. Nishio K, Okubo K, Watanabe Y, Tsuchiya T (2000) J Sol-Gel Sci Technol 19:187–191
36. Jacob MME, Arof AK (2000) Electrochim Acta 45:1701–1706
37. Srivastava N, Chandra S (2000) Eur Polym J 36:421–433
38. Lee JS, Quan ND, Hwang JM, Lee SD, Kim H, Lee H, Kim HS (2006) J Ind Eng Chem 12:175–183
39. Radev I, Georgiev G, Sinigersky V, Slavcheva E (2008) Int J Hydrogen Energy 33:4849–4855
40. Hung Y, Tawfik H, Mahajan D (2008) Systems, Applications and Technology Conference IEEE Long Island 1–5
41. Viswanath RP (2004) Int J Hydrogen Energy 29:1191–1194
42. Isa M, Ismail B, Hadzar CM, Daut I, Bakar FA (2006) Am J Appl Sci 3:2134–2135
43. Zhang J, Tang Y, Song C, Zhang J, Wang H (2006) J Power Sources 163(2006):532–537
44. Bocchetta P, Conciauro F, Quarto FD (2007) J Solid State Electrochem 11:1253–1261